

Broadband acoustic scattering with modern aesthetics from random 3D terrain surfaces generated using the Fourier Synthesis algorithm

William Henham¹, Damien Holloway² and Lilyan Panton³

¹School of Engineering and ICT, University of Tasmania, Hobart, Australia

²School of Engineering and ICT, University of Tasmania, Hobart, Australia

³School of Engineering and ICT, University of Tasmania, Hobart, Australia

ABSTRACT

Acoustic diffusers are designed to scatter sound to create diffuse sound fields, ideally providing a uniform acoustic experience over a broad frequency range within a listening space. Standard diffuser designs, such as Schroeder diffusers, while effective, may be considered by some to have a design aesthetic that does not conform to particular architectural styles. In this paper the Fourier Synthesis algorithm for procedural 3D random terrain generation is investigated as an alternative for diffuser surface geometry, providing scattering in two dimensions, and scope to vary the bandwidth through a surface smoothness parameter. The scattering properties of a prototype diffuser are investigated experimentally and through numerical modelling using a boundary element method (BEM) program called FastBEM. Good agreement between these is achieved, providing solid validation of the numerical model from which the performance of the diffuser can be assessed. The scattering properties are quantified using polar plots, 3D plots, and the diffusion coefficient. As expected, the Fourier Synthesis diffuser provides good diffusion when the wavelength of the incident sound is comparable to the wavelength of periodicity of the diffuser geometry. A preliminary investigation into the performance of the diffuser for various levels of surface roughness is made, showing that high diffusion can be extended to higher frequencies by increasing the surface roughness of the diffuser.

1. INTRODUCTION

A diffuse sound field is a sound field that has an equal distribution of energy within its volume. Acoustic diffusers are objects designed to enhance the acoustic performance of new or existing spaces by providing a surface geometry that scatters reflected sound. In doing so, the diffuser may reduce the negative effects of coherent artefacts that can be detected by the listener within a performance space, such as comb filtering, dead spots and distracting echoes in the auditorium (Cox & D'Antonio, 2009). While it is possible to treat these negative qualities with acoustic absorption it is often preferable to use acoustic diffusers, for example in large music performance spaces where significant loss of sound energy may be undesirable. An optimum degree of diffusion can enhance the listening experience.

Early diffuser designs, developed by Manfred Schroeder, consist of wells of different depth, relying on interference of reflections incorporating pseudo-random phase changes. They use a random number sequence, such as the quadratic residue sequence, to develop the geometry of the diffuser (Schroeder, 1975). While this has been shown to be effective, it represents a distinctive design aesthetic. Advances in numerical techniques give scope for the design of acoustic diffusers consistent with alternative and evolving architectural styles of modern spaces.

Procedural terrain generation may provide a suitable avenue for a refreshed acoustic diffuser design. Specifically, the Fourier Synthesis method for creating the acoustic diffuser geometry is investigated. Geometries developed using this method are both tessellating (i.e. opposite boundaries conform) and are fractal (i.e. they are self-similar upon magnification). Tessellated diffusers (i.e. multiple blocks) may be used to cover a larger area in an actual performance space, and while an investigation of the diffusing properties of such an implementation (for example, how the diffusion is enhanced or degraded) has not been investigated in this work it would be a logical next step. Based on the principle that sound waves are most effectively scattered off surface of comparable size to the sound wavelength (Everest & Pohlmann, 2009), the Fourier Synthesis diffuser offers a promising design solution due to the potential for the geometry to have both large and small features superimposed on the same geometry. Additionally, the design incorporates curved surfaces and so presents an alternative to existing designs.

In this work an acoustic diffuser panel is generated using the Fourier Synthesis technique and is investigated

experimentally for the sound scattering properties of its surface. A numerical model is developed using a boundary element method solver (FastBEM) to replicate the experiment and, once validated, is used to further investigate the acoustic diffuser geometry, in particular the effect of increasing the surface roughness of the diffuser and an investigation of the reflected sound field in three dimensions. Based on these preliminary investigations it is concluded that there is potential in the design to be used as an alternative to existing acoustic diffusers.

2. THE FOURIER SYNTHESIS ALGORITHM FOR PROCEDURAL RANDOM TERRAIN GENERATION

Acoustic diffusers generally aim to produce both spatial and temporal diffusion. Schroeder diffusers achieve both objectives effectively by use of wells of varying depth, producing a range of phase shifts in the reflected sound. The idea of the Fourier Synthesis surface is to achieve similar features using a smooth continuous surface. It has no discrete wells, so provides less control over the reflected wave phase, but achieves additional scattering of higher frequencies via the slope of the surface. Furthermore, its fractal properties mean that it contains features of all scales, hence potentially provides scattering of all frequencies, and these frequency distributions can be varied by applying appropriate filters on the various wavelength components of the surface geometry.

The Fourier Synthesis (FS) algorithm belongs to a class of procedural random terrain generation algorithms. Many of these were developed to provide terrains in computer games. Other such algorithms, such as the diamond square algorithm, have been studied as acoustic diffusing surfaces (Farner, 2014), but the FS algorithm offers advantages such as greater control over features through use of filters, infinitely differentiable continuity at opposing edges to allow perfect tessellation, and quicker computation times for large surfaces.

The algorithm used is adapted from one proposed by LaBoitaeux (2014). A surface depth matrix (\mathbf{D}) is generated by a three step process starting with a random matrix (\mathbf{A}), transforming it to wavenumber space (\mathbf{B}), filtering for the desired wavelengths and symmetry (\mathbf{C}) and transforming back to the physical spatial domain. It begins with an $M \times N$ matrix \mathbf{A} of standard normally distributed (as distinct from uniformly distributed) random numbers, i.e. with mean 0 and standard deviation 1. This is converted to wavenumber space by a 2D Discrete Fourier Transform (2D-DFT),

$$B_{k,l} = \sum_{n=0}^{N-1} \sum_{m=0}^{M-1} A_{m,n} e^{-2i\pi\left(\frac{mk}{M} + \frac{nl}{N}\right)}.$$

A pink noise filter is applied to a quarter of the matrix to attenuate the short wavelength components,

$$C_{k,l} = \frac{K}{c_{k,l}^{\alpha/2}} B_{k,l}$$

for $k \leq M/2$ and $l \leq N/2$, where K is an arbitrary scaling constant, $c_{k,l} = \sqrt{\left(\frac{k}{M}\right)^2 + \left(\frac{l}{N}\right)^2}$, and α is a ‘smoothing parameter’. The remaining three quarters of the matrix are discarded and replaced by reflection to give a symmetric matrix, which ensures that the surface tessellates when converted back to the spatial domain by an inverse 2D-DFT,

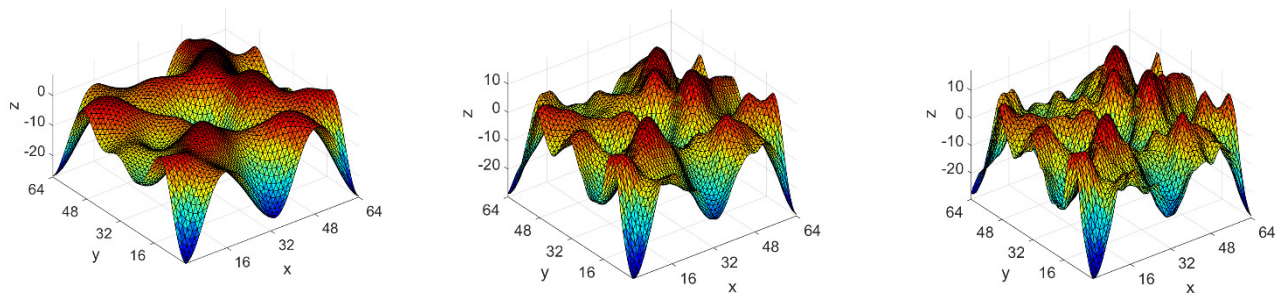
$$D_{m,n} = \frac{1}{MN} \sum_{l=0}^{N-1} \sum_{k=0}^{M-1} C_{k,l} e^{2i\pi\left(\frac{mk}{M} + \frac{nl}{N}\right)}.$$

Matrix \mathbf{D} will in general be complex; the final surface heights are the real parts. The surface may be scaled laterally or vertically as required.

The 2D-DFT is efficiently evaluated using the Fast Fourier Transform (FFT) method, in which case it is advantageous if M and N are powers of 2. In the present work $M = N = 64$, distributed over a 400×400 mm surface.

In the above algorithm higher values of the smoothing parameter α filter out higher wavenumber (shorter wavelength) geometry components more strongly, hence produce smoother surfaces.

The algorithm was implemented in Matlab, which provides the capacity to define a ‘seeded’ random number. This means that the random number sequence (or matrix) can be reproduced. This allows the effect of the roughness parameter to be studied separately from other random effects. Figure 1 shows the parent geometry, $\alpha = 9.2$ and $k = 0.006$ and two variants with $\alpha = 6.2$ and $\alpha = 5.2$ respectively. The parent (smooth) geometry was studied both experimentally and numerically, while the rougher variants were only studied numerically.



a) Parent geometry ($\alpha = 9.2$)

b) Child geometry, increased roughness ($\alpha = 6.2$)

c) Child geometry, roughness increased further ($\alpha = 5.2$)

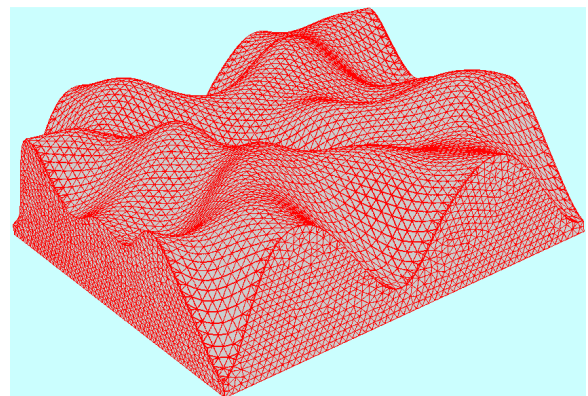
Figure 1: Diffuser geometry (parent geometry, and two variants)

3. EXPERIMENTAL PROCEDURE

The purpose of conducting a physical analysis of the sound scattering properties of the shape is primarily to provide an empirical baseline that can be used to validate the results of the numerical model. A prototype diffuser is made of layers of 18 mm MDF sheet that were cut into 400×400×18 mm sheets and glued together to form a 400×400×114 mm block. A 400 mm diffuser gives good scattering in the 1–4 kHz range (see Section 6) and was of a size that could validly be tested in the facilities available; it could easily be scaled to shift the desired design frequency range. This is then milled to produce the surface geometry of the diffuser. To achieve accurate geometry the shape is milled twice, first with a coarse cut and then with a fine cut. To achieve a glossy and highly reflective surface the geometry was treated with builder’s bog and fiberglass resin and milled for a third time to give the most accurate geometry possible (see Figure 2a).



a) Physical model



b) Computational mesh

Figure 2: Diffuser prototype used for acoustic testing.

The testing method follows the method outlined in ISO 1749-2:2012(E). Ideally, acoustic testing would be performed in an anechoic chamber, however, this standard describes an alternative, the ‘2D boundary method’, which achieves good results where anechoic facilities are unavailable. In this method, the subject is placed centrally in a large empty space with a smooth reflective floor. A microphone (or microphone array) is then placed at a constant radius from the diffuser in a measurement arc, which in this work had a radius of 4 m. A speaker is then placed at twice this radius facing directly normal to the diffuser. An impulse response is then measured.

The advantage of this setup is, assuming the space is large enough, it is possible to isolate the response of the diffuser from the response of the wall boundaries of the testing venue. If there is a significant distance between the wall boundaries and the diffuser then it follows that there will be significant time delay between the microphone registering a reflection off the diffuser and registering a response from the boundaries due to the proximity of the diffuser to the microphone relative to the walls (see Figure 4). Thus, we can window out the wall reflections and assume the floor is a perfect reflector (which means we are in essence testing the diffuser and its reflection below the floor line). Thus, accurate results are possible without the need for an anechoic chamber.

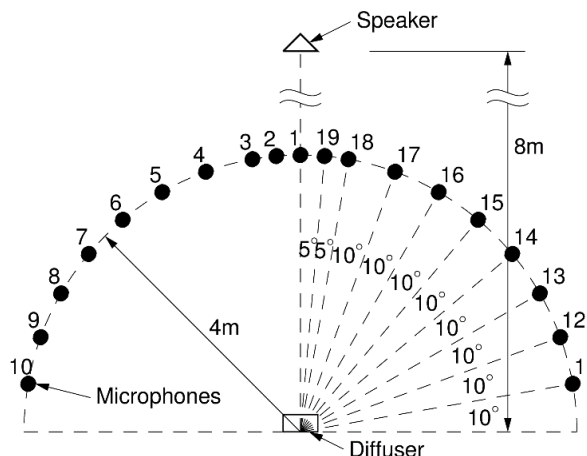


Figure 3: Diagram of microphone, diffuser and source positioning in physical test.

Once the dimensions of the test are set it is possible to define the minimum size required of the test venue using simple geometry. Specifically the minimum reflection path length from the speaker to the boundary of the space to the microphone must be at least $5R$ (20 m), to ensure that all unwanted reflections are measured as a separate impulse to the reflection from the diffuser. Details are given in ISO 1749-2:2012(E), and a school gymnasium was found to satisfy the requirements. A 60 second logarithmic sine sweep signal from 20–20,000 Hz was used, generated using a Swan M10 speaker. These were recorded using a Dayton EMM-6 mic 3810. Signals were captured and analysed using ARRAE software (Cabrera, 2014).

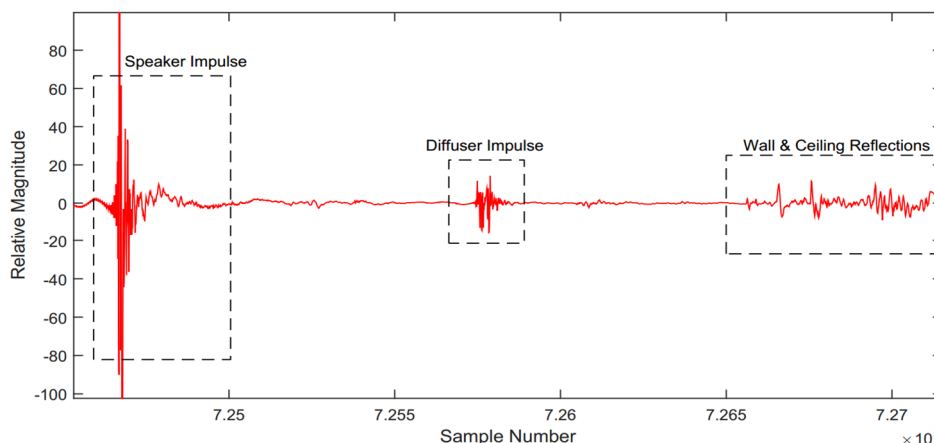


Figure 4: Impulse response of experimental setup.

Figure 4 shows a typical signal after the sine sweep has been converted to an impulse response. The speaker impulse, wall reflection and diffuser impulse are very clearly separated and the latter can be isolated, replicating anechoic conditions. By taking the difference of two signals, one with the diffuser present and one with it absent, it is possible to remove the effect of background noise on the impulse response of the diffuser (see Figure 5). Having done so, it is a simple matter of windowing the impulse response of the diffuser from the rest of the data to perform further analysis on the reflection.

Once the reflection from the diffuser is isolated, a Fourier transform is performed to analyze the frequency response of the signal. Next the frequency response of the equipment (i.e. the speaker and microphone, measured as the ‘direct sound’ with the microphone at position 1 in Figure 3, but turned to face speaker) must be deconvolved from the measured result so as to remove any colouring of the signal resulting from imperfections in the experimental equipment. Thus levels are relative and no calibration is required. By averaging the power at each location at a particular center frequency, it is possible to produce a polar plot of the reflection at that frequency, which was done for 1/3 octave averages. This is discussed in further detail in Section 5.

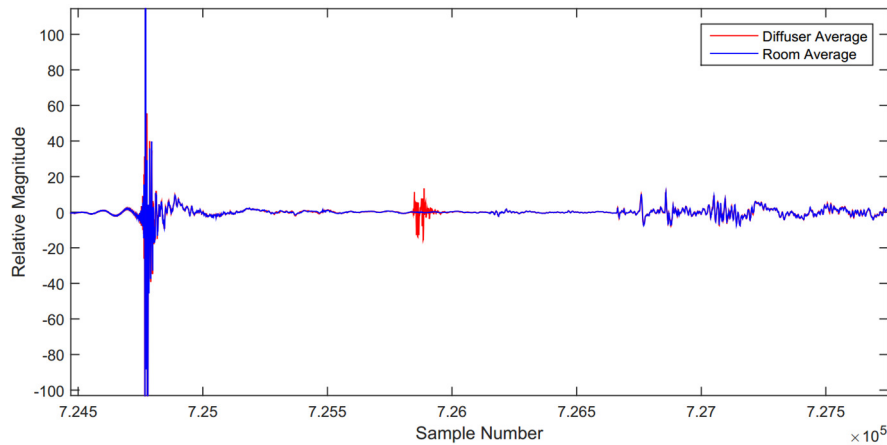


Figure 5: Response of room with (red) and without (blue) the diffuser present.

4. NUMERICAL SIMULATIONS

4.1 Objective and Method

Computational modelling of the acoustic diffuser, validated with the experimental results, provides a means to explore different designs. The most accurate models are those that solve for a potential function ϕ satisfying the Helmholtz wave equation, $\nabla^2 \phi + k^2 \phi = 0$ for wavenumber k , from which pressure $p = \rho \frac{\partial \phi}{\partial t}$ and velocity $\vec{v} = \nabla \phi$ fields are computed. It is usual to solve acoustic scattering problems (such as the performance of a diffuser) in the frequency domain, and to separate the total potential field into incident and scattered components as $\phi_{\text{Total}} = \phi_{\text{Incident}} + \phi_{\text{Scattered}}$. The incident field is the free field produced by the source in infinite space, and is known. It defines the boundary conditions required by the boundary element method (BEM) to solve the diffracted field. The scattered field thus obtained from the BEM is combined with the incident to obtain the total.

Most commonly this problem is solved using either the finite element or boundary element method (FEM or BEM). The latter uses Green's second identity to reduce the three dimensional task of solving the problem in the acoustic domain (the air space surrounding the diffuser) to a two dimensional one of solving the problem on the boundary of that domain (the diffuser surface), vastly reducing the size of the problem. It is particularly efficient for exterior problems. Further significant efficiency gains are made by modelling the floor on which the diffuser is placed (assumed to be a hard reflective surface) as a symmetry plane, requiring a 'mirror image' of the diffuser, rather than representing the floor surface.

Based on thorough testing in previous work, the commercial BEM program FastBEM Acoustics was chosen as an efficient and accurate BEM solver for this purpose (Wall, 2014), (Panton, 2014). However, other programs were required for pre- and post-processing as described below. FastBEM offers a full conventional BEM and three alternative solvers that provide various degrees of approximation to the conventional BEM. The alternative solvers include *Adaptive Cross Approximation (ACA)*, *Fast Multipole Method (FMM)*, and *High Frequency (HF)* (FastBEM, 2016). Investigations by both Wall (2014) and Panton (2014), using similar scenarios to those explored in this work, showed excellent agreement between FastBEM's conventional solver and ACA solver, as well as with other BEM and FEM software (ABEC and ANSYS respectively). The conventional solver in FastBEM and the solver used by ABEC and ANSYS, solve the Helmholtz equation without approximation and thus can be considered to be the most reliable. The FMM and HF solvers, while more efficient, involve approximations to the Helmholtz equation and their results were found to deviate significantly from the conventional solvers at high frequencies (Panton, 2014). While they were much quicker they were deemed insufficiently accurate for the problem posed in this paper. The conventional solver used more memory than the ACA solver, but was chosen as the ACA proved unreliable because it did not always converge to a solution, and was more susceptible to anomalous or irregular frequencies (see Section 4.3).

As well as using the full conventional solver in FastBEM, the element size was fixed by the Fourier Synthesis algorithm grid spacing. This was chosen to give 6.8 elements per wavelength at 8 kHz (the highest frequency), which would be sufficiently fine for highest frequency studied, and more than sufficient for the lower frequencies studied. Together these choices ensure the high accuracy of results presented in this paper. Another major factor in

obtaining accurate results is mesh quality. FastBEM does not have a built-in mesher and a predefined mesh must be imported into the program. The method used for geometry meshing is described below in the next section.

4.2 Modelling Process

The basic diffuser surface geometry was created in Matlab as a matrix of heights defined on a uniform two-dimensional grid. These were very easily triangulated in a perfectly regular pattern by inserting diagonals across the grid squares, producing a good quality mesh on the front face of the diffuser. Depending on the resolution required, this could be arbitrarily fine, and always regular. However it proved much more difficult to obtain a regular mesh on the sides and back of the diffuser.

Unfortunately the STL format solid model file generated by Matlab, though ideal for manufacture, defined triangles on the body sides with height equal to the full local height of the diffuser. These were therefore of very high aspect ratio. While this was not an issue in the manufacture of the physical model since these surfaces were perfectly flat, they violated the requirement in BEM modelling that the element size must be significantly smaller than the wavelength. Even after subdividing the elements (using an open source meshing program called Gmsh) it was very difficult to avoid high aspect ratio elements, which are known to be very poor for numerical simulation. Testing confirmed results to be very poor with this mesh.

The solution was to convert the STL output from Matlab into a format that could be read by the more sophisticated meshing program ANSYS, which was used to produce a high quality mesh. Prior to reading into ANSYS the STL geometry had to be stitched together as a solid geometry. The 3D modelling and rendering software 3DS Max (produced by Autodesk) was used for this purpose, outputting a SAT file, a standard solid geometry format. ANSYS APDL was then used to create a mesh and output it in the desired format using the procedure recommended by FastBEM distributors (FastBEM, 2016). The FastBEM input files were also edited to ensure all the correct inputs; namely, the desired speed of sound, frequency range and frequency increment. A critical step in the process was to ensure that the element normals were all pointing in the correct direction, namely out of the acoustic domain (i.e. into the diffuser body) as required by FastBEM for the correct solution, which was not the default setting in ANSYS. The final mesh produced is shown in Figure 2b.

A final step was to generate the 'field points' (i.e. 'receiver points'), the locations at which the solution was sought. These were the microphone locations in physical experiment, a semi-circle of radius 4 m on the $z = 0$ plane, but in 1° increments, and were generated using a C# script developed by Wall (2014). A second set of field points were used for the 'explosion plots' (see Figure 11) defined on a hemisphere of radius 4 m.

The sound source, as in the experiments, was located 8 m in front of the diffuser. The source height made a significant difference to the results because of the pattern of constructive and destructive interference as a function of frequency. Although the speaker was nominally on the ground plane, the center of the speaker cone was at a height of 53 mm, which was faithfully replicated in the numerical model. To maintain symmetry (to model the ground plane) an identical image source was located at -53 mm. A monopole source was used. Although the speaker was not omnidirectional, the only sound of relevance in these experiments after processing was that which was reflected off the diffuser, so it is sufficient in comparing numerical and experimental results that the speaker performance did not vary over the very small solid angle subtended by the diffuser face.

4.3 Outputs

As mentioned above, the total sound field can be decomposed into incident and scattered fields. FastBEM only outputs the total pressures, however scattered pressures were output from the experiments and are also required for calculating diffusion coefficients. Therefore, before plotting results the incident field had to be calculated and subtracted from the total to isolate the scattered. This additional processing was done in Matlab. FastBEM defines pressure from a monopole source at a distance r as $p(r) = \hat{Q} \frac{e^{ikr}}{4\pi r}$, where \hat{Q} is the complex source strength, set to 4π (with no imaginary part) for all tests. This was calculated for both the source and its image, and it was necessary that subtraction was performed using the complex total and incident pressures to retain the relative phase information.

Pressures were obtained thus for frequencies from 20 Hz – 20 kHz in $1/12^{\text{th}}$ octave steps below 2 kHz, and in $1/24^{\text{th}}$ octave steps above 2 kHz, and on the observation semicircle at spatial increments of 1° . Further post-processing to produce the polar plots and diffusion coefficient plots was done in the same manner as for the experimental results. Using the numerical results, it was possible to investigate the sensitivity to angular position.

It is known that BEM models have irregular frequencies corresponding to eigenvalues of the coefficient matrix where the solution degenerates. One such irregular solution was found at 2378 Hz. As shown in Figure 6 this was confirmed to be anomalous by solving the problem in this vicinity at a much finer frequency increment, showing that the response was otherwise smooth and well behaved either side. These irregular frequencies can be thought of as non-physical internal resonances, and can be shifted by defining cavities inside the body, which obviously have no effect on the exterior solution (Lock, 2014). However, in the present work the frequency response curves were sufficiently smooth that the anomalous result could be neglected and replaced with an interpolated value.

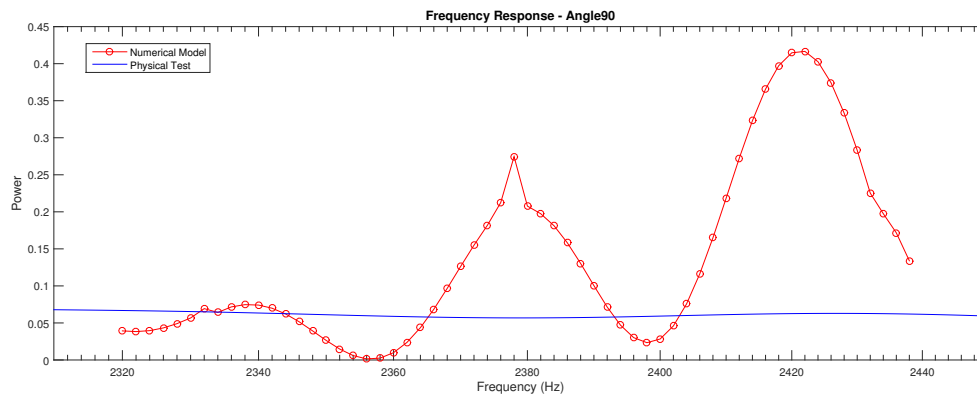


Figure 6: A plot of power versus frequency between 2320-2400 Hz, demonstrating an irregular solution at 2378 Hz.

5. VALIDATION

The experimental results were used to validate the BEM model before using the latter to explore diffuser geometry. Initial validation considered the frequency response at individual measurement locations. A typical example, Figure 7, shows the scattered power fraction at 120°.

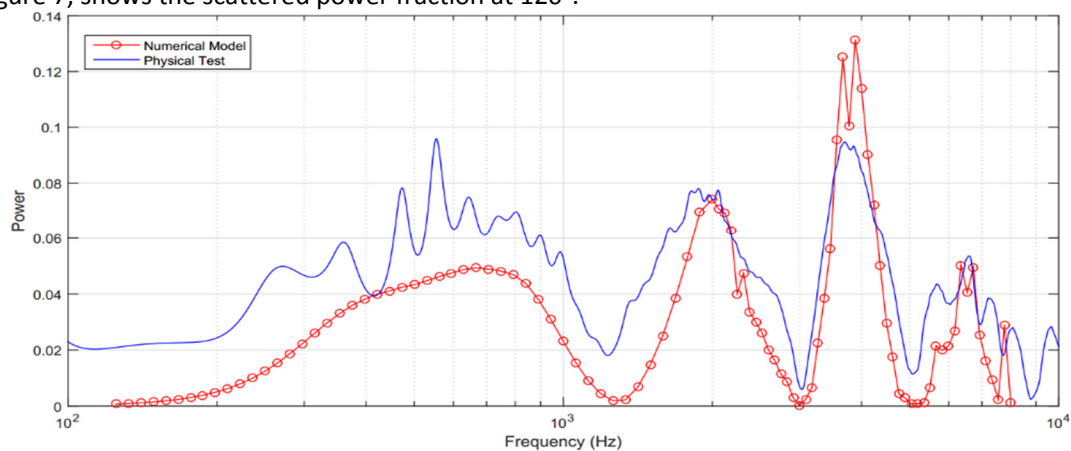


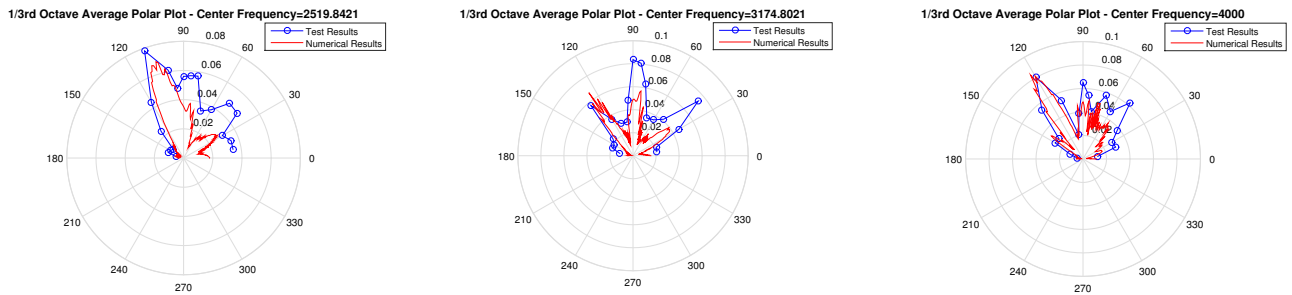
Figure 7: Comparison of numerical model and experimental results at 120°.

The two sets of results are remarkably similar, at least in the trend of the data if not in the exact value of the power at each frequency. However, there are clear differences, particularly at low frequencies. This is likely to be due to the limitations of the test setup, significant low frequency background noise due to the location, a school gymnasium near a main road. This is further exacerbated because the speaker used was designed for mid frequencies, and the diffuser is effectively ‘invisible’ at these wavelengths, so the overall level of the measured signal at low frequencies was very low. The fact that at low frequency the experimental polar plots (not reproduced here) were quite random and always greater than the computed one supports this background noise hypothesis.

The range of best agreement was 2–5 kHz. This was true for all measurement locations; therefore, when producing a polar response plot for the sake of comparing the numerical and experimental data, it is favourable to investigate this region. This is also the range of frequencies of most interest, where the diffuser performs best. Examples of typical plots are given in Figure 8 showing the polar response at center frequencies 2520, 3175 and

4000 Hz. Again, while the exact numerical values of the sound power do not match at every point what is important to note is that the gross features of the data are consistent between the numerical model and the experiment. This gives confidence in the numerical model, and illustrates what can be achieved with the experimental results with limited equipment using the 2D boundary method for measuring sound scattering off surfaces.

Above 6 kHz the wavelength is such that results are very sensitive to small changes in measurement location, and the element size to wavelength ratio is approaching the limits of the acceptable range, so it is not surprising that the agreement degrades.



a) Center frequency = 2520 Hz

b) Center frequency = 3175 Hz

c) Center frequency = 4000 Hz

Figure 8: Polar response plot of measured and numerical scattered sound

6. GEOMETRY EXPLORATION USING VALIDATED MODEL

Following the validation of the BEM model with the experimental results, different diffuser geometries could be investigated. In particular, the surface roughness was varied, and the impact on diffuser quality investigated. In theory, because the rougher shape has both large and small undulations it should provide good diffusion for a broader range of frequencies than the smoother diffuser. A diffusion coefficient was found in accordance with ISO 17497-2:2012(E), normalised relative to the diffusion properties of a flat plate. The normalised diffusion coefficients were calculated from the response on a semicircle around the diffuser, to match the experimental setup. Numerical results could alternatively be integrated over a hemisphere to quantify scattering in two dimensions, but these are not presented here.

In Figure 1 the parent geometry ($\alpha = 9.2$) was shown, and the two variants studied (corresponding to $\alpha = 6.2$ and $\alpha = 5.2$ respectively). In Figure 9 the normalised diffusion coefficient is plotted against frequency for these. At 1 kHz all three diffuser begin to provide some level of diffusion; this corresponds to the largest sized undulations in the diffuser geometry. Between 1 kHz and 8 kHz surface roughness has a significant effect on the normalised diffusion coefficient. As expected, the smoothest surface ($\alpha = 9.2$) provides the best diffusion at lower frequency (1–1.5Hz), while at slightly higher frequencies (2–3.1 kHz) the roughness surface ($\alpha = 5.2$) shows significantly better diffusion. The diffuser geometry with smoothness corresponding to $\alpha = 6.2$ appears to show somewhat of a compromise between the two extremes, with a less varied diffusion coefficient over the entire frequency range.

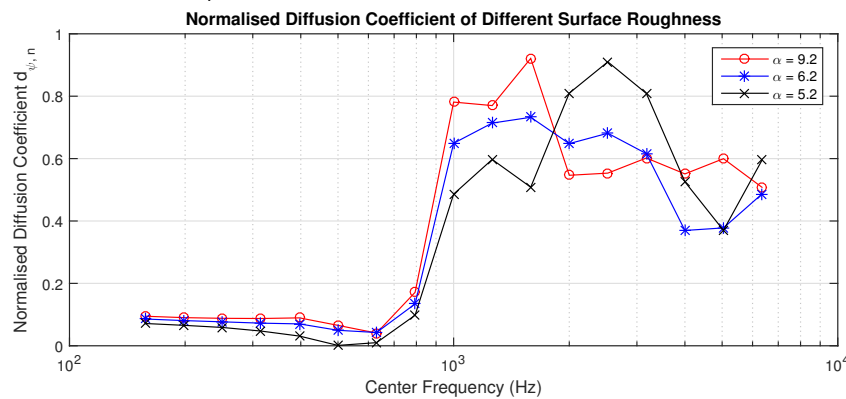


Figure 9: Normalised diffusion coefficient versus center frequency for the three diffuser geometries investigated ($\alpha = 9.2$, $\alpha = 6.2$ and $\alpha = 5.2$).

To further investigate the diffusion properties of each surface geometry polar plots are presented at frequencies of interest. Figure 10a shows the 1260 Hz 1/3rd octave band. We see that for each diffuser geometry there is a specular reflection; however, for the smoothest diffuser surface the magnitude of this reflection is significantly reduced compared to the rougher surfaces. Figure 10b shows the 2000 Hz 1/3rd octave band; we see that a significant lobe occurs at around 110° for the smoothest diffuser ($\alpha = 9.2$), whereas for the intermediate diffuser geometry there are two smaller lobes. The roughest diffuser shows no significant lobes; the energy is more evenly spread over all angles, which corresponds to a significantly higher diffusion coefficient than the smoother diffuser geometries.

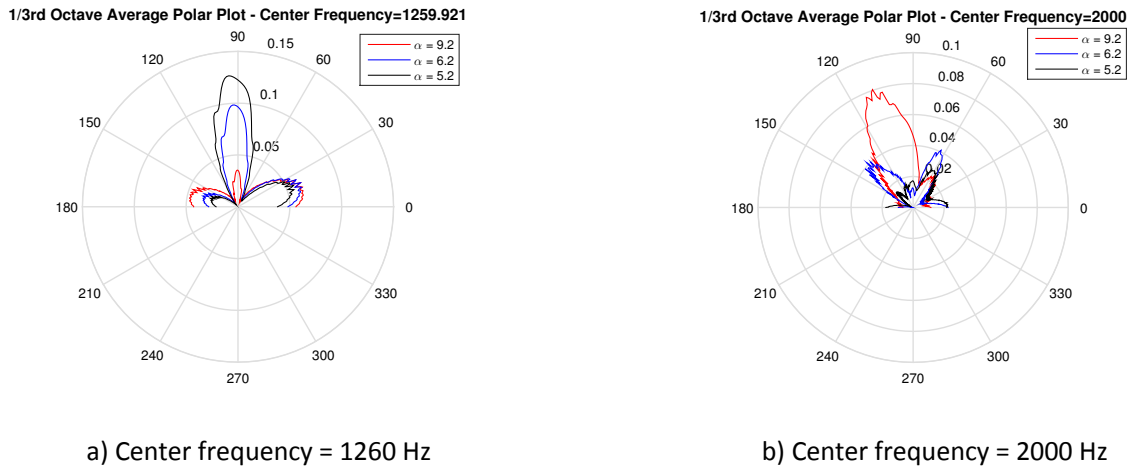


Figure 10: 1/3rd octave average polar plot

Since the diffuser geometry has a variation in 3D, rather than 2D, measurements made on a single arc may not be fully representative of the scattered sound field of the diffuser, so scattering over a hemisphere was investigated in Figure 11. For this test the source was placed directly central to the diffuser face at a distance of 8 m, and the hemisphere has a radius of 4 m. The sound pressure on the hemisphere has been plotted as a 3D ‘explosion plot’ shown in Figure 11a; for reference the corresponding plot is shown for a flat plate in Figure 11b. This demonstrates that the diffuser provides a high level of diffusion in 3 dimensions, but the lobes of scattered sound point out in many directions, confirming that diffusion coefficient based on measurements on a circular arc may in theory differ significantly at times from one based on measurements over a hemisphere.

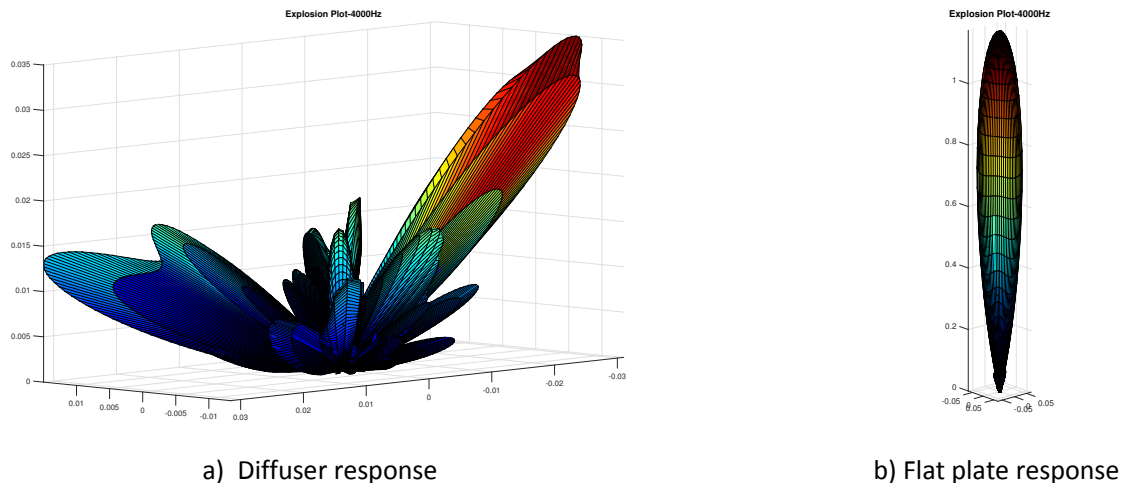


Figure 11: Explosion plot at 4000 Hz for diffuser and flat plate.

Overall, it appears that while at higher frequencies the rougher diffuser surface provides significantly improved diffusion, at the lower frequencies the introduction of more surface roughness impacts the gross features of the

diffuser terrain (which are equivalent to the wavelength at 1–1.5 kHz) and thus reduces the level of diffusion occurring. Notably a compromise can be reached by using an immediate roughness ($\alpha = 6.2$) which provides a reasonable level of diffusion over 1–3 kHz.

7. CONCLUSIONS

An experimental investigation has validated the use of BEM modelling of random terrain surface diffusers, which subsequently has been used to investigate the diffusion properties of several random terrain diffuser geometries. As expected, Fourier Synthesis diffusers provide good diffusion when the wavelength of the incident sound is comparable to the wavelength of periodicity of the diffuser geometry. A preliminary investigation into the performance of the diffuser for various levels of surface roughness has shown that improved diffusion can be extended to higher frequencies by increasing the surface roughness of the diffuser. Future work could further investigate random terrain diffusers, in particular it would be beneficial also to study scattering over a hemisphere, the impact of altering the random number seed, the vertical scale, and the value of N in the Fourier Synthesis. This study also was limited to a single diffuser; however, a logical next step would be investigating a tessellated array of diffusers, as would more likely be used in a room.

ACKNOWLEDGEMENTS

The authors would like to thank Peter Seward for building the diffuser prototype and Jack Pitt for his assistance in undertaking the experimental testing component of this work.

REFERENCES

- Cabrera, D, Jimenez, D & Martens, W 2014, 'Audio and Acoustical Response Analysis (AARAE): a tool to support education and research in acoustics' *Proceedings of the 43rd International Congress on Noise Control Engineering*, Melbourne, Australia
- Cox, TJ & D'Antonio, P 2009, *Acoustic Absorbers and Diffusers - Theory Design and Application*, 2nd edn, Taylor and Francis.
- Everest, FA & Pohlmann, KC 2009, *Master Handbook of Acoustics*, 5th edn, McGraw Hill.
- Farner, J 2014, 'Acoustic diffusion: Simulation and Investigation of 2D Diffusers using the Boundary Element Method', BE (Hons) thesis, University of Tasmania, Hobart.
- FastBEM 2016, 'FastBEM Acoustics, User Guide', Advanced CAE Research, Cincinnati, Ohio, USA.
- International Organization for Standardisation 2012, *Acoustics - Sound Scattering Properties of Surfaces - Part 2: Measurement of Directional Diffusion Coefficient in a Free Field*, 17497-2:2012, International Organization for Standardisation, Switzerland, Geneva.
- LaBoitaeux, C 2014, *Fast Fourier terrain generation*, viewed 30 Sep 2016, <<https://sites.google.com/site/curtislaboiteaux/projects/fast-fourier-terrain-generation>>
- Lock, A 2014, 'Development of a 2D Boundary Element Method to Model Schroeder Acoustic Diffusers', BE(Hons) thesis, University of Tasmania, Hobart.
- Panton, L and Holloway, D 2014, 'A BEM study of the influence of musicians on onstage sound fields measures in auditoria' *Proceedings of the 43rd International Congress on Noise Control Engineering*, Melbourne, Australia.
- Schroeder, MR 1975, 'Diffuse Sound Reflection by Maximum Length Sequence', *Journal of Acoustical Society America*, vol 57, no.1, pp. 149-150.
- Wall, D 2014, 'Analysis of Acoustic Software', BE thesis, University of Tasmania, Hobart.